

Molecular Dynamics Simulations of End-to-End Contact Formation in Hydrocarbon Chains in Water and Aqueous Urea Solution

Raymond D. Mountain*[†] and D. Thirumalai^{†,‡}

Contribution from the Physical and Chemical Properties Division,
National Institute of Standards and Technology, Gaithersburg, Maryland 20899-8380,
and IPST, University of Maryland, College Park, Maryland 20742

Received April 5, 2002; E-mail: RMountain@nist.gov

Abstract: We probe the urea-denaturation mechanism using molecular dynamics simulations of an elementary “folding” event, namely, the formation of end-to-end contact in the linear hydrocarbon chain (HC) $\text{CH}_3(\text{CH}_2)_{18}\text{CH}_3$. Electrostatic effects are examined using a model HC in which one end of the chain is positively charged (+0.2e) and the other contains a negative charge (−0.2e). For these systems multiple transitions between “folded” (conformations in which the chain ends are in contact) and “unfolded” (end-to-end contact is broken) can be observed during 4 ns molecular dynamics simulations. In water and 6 M aqueous urea solution HC and the charged HC fluctuate between collapsed globular conformations and a set of expanded structures. The collapsed conformation adopted by the HC in water is slightly destabilized in 6 M urea. In contrast, the end-to-end contact is disrupted in the charged HC *only in aqueous urea solution*. Despite the presence of a large hydrophobic patch, on length scales on the order of $\sim 8\text{--}10\text{ \AA}$ “denaturation” (transition to the expanded unfolded state) occurs by a direct interaction of urea with charges on the chain ends. The contiguous patch of hydrophobic moieties leads to “mild dewetting”, which becomes more pronounced in the charged HC in 6 M aqueous urea solution. Our simulations establish that the *urea denaturation mechanism is most likely electrostatic in origin*.

1. Introduction

The purpose of this paper is to probe contact formation between two ends of model hydrocarbon chains in water and 6 M aqueous urea solution. We undertook this study primarily to obtain an understanding, at the molecular level, of the function of urea in disrupting the structure of proteins. The simulations reported here may also be useful in providing insights into the end-to-end contact formation in peptides.^{1,2}

The most common way of unfolding proteins is by adding excess amounts of denaturants such as urea or guanidinium hydrochloride. Because *in vitro* refolding experiments are often initiated by first chemically unfolding proteins, it is necessary to understand the way proteins are denatured and the nature of the resulting states. Despite extensive work, the molecular mechanism by which urea unfolds proteins is not fully understood.³ Two different mechanisms have been proposed to explain the way urea denatures proteins.

1.1. Hydrophobic Mechanism. Pioneering transfer experiments by Nozaki and Tanford⁴ showed that the solubilities of side chains of amino acids are greater in aqueous urea solutions

than in water. This led to the proposal that the increase in the exposed surface area upon urea-induced unfolding leads to the enhanced stability of the unfolded protein. The free energy gain, upon unfolding, may be written as $\Delta G(C) \approx -\gamma(A_U - A_N)$, where C is the concentration of urea, γ is the surface tension, and A_U and A_N are the solvent-accessible surface areas of the residues in the unfolded (U) and the folded (N) states, respectively. Since $A_U > A_N$ (especially for the usually buried hydrophobic residues), it follows that the unfolded state has a lower free energy in high urea concentration. The denaturation mechanism is attributed to the effective solvation of hydrophobic residues in aqueous urea solution.

1.2. Electrostatic Mechanism. A different proposal, inferred from experiments involving only the peptide backbone,⁵ posits that denaturation occurs by direct interaction of urea with the peptide backbone and/or the polar and charged residues. Thus, urea is directly engaged in hydrogen bonding with both backbone and side chains so that the denaturation mechanism is “electrostatic” in origin. This proposal, which is supported by simulations using simple model systems,⁶ is also attractive from the perspective of kinetics of urea denaturation. This is because the solvent-exposed polar and charged residues can initially hydrogen bond with urea, leading to the destabilization of the native structure. Thus, in the direct interaction (or

[†] National Institute of Standards and Technology.

[‡] University of Maryland.

(1) Bieri, O.; Wirz, J.; Hellrung, B.; Schutkowski, M.; Kiefhaber, T. *Proc. Natl. Acad. Sci. U.S.A.* **1999**, *96*, 9597.

(2) Lapidus, L. J.; Eaton, W. A.; Hofrichter, J. *Proc. Natl. Acad. Sci. U.S.A.* **2000**, *97*, 7220.

(3) Shortle, D.; Dill, K. A. *Annu. Rev. Biochem.* **1991**, *60*, 795.

(4) Nozaki, Y.; Tanford, C. *J. Biol. Chem.* **1963**, *238*, 4074.

(5) Robinson, D. R.; Jencks, W. P. *J. Am. Chem. Soc.* **1965**, *87*, 2462.

(6) Wallqvist, A.; Covell, D. G.; Thirumalai, D. *J. Am. Chem. Soc.* **1998**, *120*, 427.

electrostatic) mechanism denaturation proceeds from the outside. Additional destabilization of the folded proteins undoubtedly arises due to the preferred solvation of the buried hydrophobic residues in aqueous urea solution.

Because of the small free energy differences involved in protein denaturation, it has been difficult to experimentally establish the validity of either mechanism. The typical loss in free energy upon denaturant-induced unfolding of proteins is between -5 and -15 kcal/mol. For example, the ΔG_{NU} per residue for CI2 (a small protein with 64 amino acid residues) is only -75 cal/mol.⁷ Thus, it is difficult to distinguish between the two mechanisms using experiments alone. Although transfer experiments show that urea enhances the solubilities of both polar and nonpolar moieties, urea-induced denaturation is almost always discussed only in terms of the hydrophobic mechanism thanks in part to the series of important studies by Tanford.^{4,8} It is not known which of the two mechanisms is dominant in denaturing proteins.

Insights into the denaturation process may be obtained using molecular dynamics simulations. Previous studies^{6,9,10,11} have focused on the effect of urea on the thermodynamics of hydrophobic interactions. The neglect of internal structure in the solutes^{6,11} prevents the assessment of chain entropy effects on the mechanism of urea denaturation. Straightforward molecular dynamics (MD) simulation of urea-induced unfolding of even small proteins, at ambient conditions, is not possible because the unfolding times of proteins far exceed microseconds. Because such simulations are fraught with sampling problems, unusually high temperatures are often used to unfold proteins.¹² Even under these harsh conditions multiple folding/unfolding simulations are not observed.

1.3. Simulations. To minimize the sampling problems, we performed MD simulations of a linear aliphatic chain, $\text{CH}_3\text{-(CH}_2)_n\text{CH}_3$ with $n = 18$. Studies probing the solvation of alkanes¹³ are useful in understanding the nature of hydrophobic interaction.¹⁴ Water is a poor solvent for the hydrocarbon chain, and hence, it is expected that for sufficiently large n the chain will adopt a globular conformation. Explicit simulations show that linear hydrocarbon chains with n as high as 12 are relatively extended in water.^{15,16} The minimum value of n can be estimated using a Flory-like argument. By balancing the energy gain due to the favorable van der Waals attraction between the methyl groups and the penalty for creating a certain number of bonds that have to be in the *gauche* conformation for the chain to fold, we estimate that for $n \geq 15$ the globular state is free energetically preferred in water. Our choice of $n = 18$ is based on computational efficiency, and the possibility of inducing sufficient *gauche* defects in the dihedral angles to induce contacts between the nonbonded CH_3 groups at the chain ends. To investigate the role of electrostatic interactions in the

denaturant-induced unfolding of proteins, we also consider a model system in which charges are placed on the CH_3 groups at the ends of the chain. Comparing the responses of the two systems enables us to shed light on the mechanisms of urea-induced denaturation and, in a limited way, on the dynamics of contact formation in real chains.

2. Computational Methods

2.1. Models. Intermolecular interactions are modeled using standard site-site potentials. The pair potentials include partial charges and Lennard-Jones (LJ) interactions. The charges are located on the centers of the atoms. Site-site interaction between molecules i and j , with R denoting collectively the coordinates of the molecule, is given by

$$V(R_i, R_j) = \sum_{\alpha \in i, \beta \in j} \frac{C_{\alpha\beta}^{12}}{r_{\alpha\beta}^{12}} - \frac{C_{\alpha\beta}^6}{r_{\alpha\beta}^6} + \frac{q_\alpha q_\beta}{4\pi\epsilon_0 r_{\alpha\beta}} \quad (1)$$

where $r_{\alpha\beta}$ is the scalar distance between sites α and β . With this standard parametrization the interaction between molecules is fully specified in terms of the LJ potentials and the partial charges q_α .

2.2. Water. We use the three-site rigid SPC/E model¹⁷ for water. In this model of the water molecule, the hydrogen atoms are at a distance 0.1 nm from the oxygen site and the HOH angle is 109.47°. The charges on oxygen and hydrogen are $q_{\text{O}} = -0.8476e$ and $q_{\text{H}} = 0.4238e$, respectively. The LJ parameters for the oxygen sites are $\epsilon_{\text{O}} = 0.1548$ kcal/mol and $\sigma_{\text{O}} = 0.3166$ nm.

2.3. Urea. The OPLS force field, introduced by Duffy et al.,¹⁸ is used for urea, $(\text{NH}_2)_2\text{CO}$. The LJ parameters for carbon, oxygen, nitrogen, and hydrogen are (kcal/mol) $\epsilon_{\text{C}} = 0.105$, $\epsilon_{\text{O}} = 0.210$, $\epsilon_{\text{N}} = 0.170$, and $\epsilon_{\text{H}} = 0$, respectively. The LJ σ values are $\sigma_{\text{O}} = 0.296$ nm and $\sigma_{\text{N}} = 0.325$ nm. Partial charges are $q_{\text{C}} = 0.142e$, $q_{\text{O}} = -0.390e$, $q_{\text{N}} = -0.542e$, and $q_{\text{H}} = 0.333e$. Hydrogen atoms are 0.1 nm from N. The NC and CO bond lengths are 0.135 and 0.1265 nm, respectively. The angles between NCO and CNH are 121.4° and 120°, respectively.

2.4. Hydrocarbon. Following our previous study,¹⁶ we used a united atom, site-site interaction model for the linear alkane chain $\text{CH}_3(\text{CH}_2)_n\text{-CH}_3$ with $n = 18$. The intramolecular force field for the hydrocarbon chain can be decomposed into $V_{\text{intra}} = V_2 + V_3 + V_4 + V_5$. The first two terms correspond to harmonic bond stretching and harmonic bond angle potential. The term V_4 contains the torsion interactions involving four consecutive sites. The V_5 term represents nonbonded interactions between sites that are separated by three or more sites. The nonbonded terms are modeled using Lennard-Jones potentials. The parameters for the HC force field are given elsewhere.¹⁶ In some cases, a partial charge of 0.2e was placed on one of the CH_3 sites and a compensating charge of $-0.2e$ was placed on the other CH_3 site. This was done to examine the role of electrostatics in determining the structure of the chain in the presence of urea.

2.5. Simulation Details. The system consisted of 8000 solvent molecules plus 1 alkane chain molecule. Aqueous urea solution was obtained by removing an appropriate number of water molecules and replacing them by urea. The solvent molecules were treated as rigid objects, and the orientational degrees of freedom of the solvent molecules were described by quaternions.^{19–21} The equations of motion were integrated using an iterated form of the Beeman algorithm^{22,23} with a time step of 1 fs. The interactions were smoothly set to zero at

- (7) Itzhaki, L. S.; Otzen, D. E.; Fersht, A. R. *J. Mol. Biol.* **1995**, *254*, 260.
 (8) Tanford, C. *The Hydrophobic Effect—Formation of Micelles and Biological Membranes*; Wiley-Interscience: New York, 1973.
 (9) Vanzi, F.; Madan, B.; Sharp, K. *J. Am. Chem. Soc.* **1998**, *120*, 10748.
 (10) Chitra, R.; Smith, P. E. *J. Phys. Chem. B* **2000**, *104*, 5854.
 (11) Ikeguchi, M.; Nakamura, S.; Shimizu, K. *J. Am. Chem. Soc.* **2001**, *123*, 677.
 (12) Tirado-Rives, J.; Orozco, M.; Jorgensen, W. L. *Biochemistry* **1997**, *36*, 7313.
 (13) Gallichio, E.; Kubo, M. M.; Levy, R. M. *J. Phys. Chem. B* **2000**, *104*, 6271.
 (14) Hummer, G.; Garde, S.; Garcia, A. E.; Pratt, L. R. *Chem. Phys.* **2000**, *258*, 349.
 (15) Wallqvist, A.; Covell, D. G. *Biophys. J.* **1996**, *71*, 600.
 (16) Mountain, R. D.; Thirumalai, D. *Proc. Natl. Acad. Sci. U.S.A.* **1998**, *95*, 8436.

- (17) Berendsen, H. J. C.; Grigera, J. R.; Straatsma, T. P. *J. Phys. Chem.* **1987**, *91*, 6269.
 (18) Duffy, E. M.; Severance, D. L.; Jorgensen, W. L. *Isr. J. Chem.* **1993**, *33*, 323.
 (19) Evans, D. J.; Murad, S. *Mol. Phys.* **1977**, *34*, 327.
 (20) Sonnenschein, R. *J. Comput. Phys.* **1985**, *59*, 347.
 (21) Rapaport, D. C. *J. Comput. Phys.* **1985**, *60*, 306.
 (22) Schofield, P. *Comput. Phys. Commun.* **1973**, *5*, 17.
 (23) Mountain, R. D.; Brown, A. C. *J. Chem. Phys.* **1985**, *82*, 4236.

about 10 Å using the shifted force method²⁴ with one important exception. The exception is the Coulomb interaction between the partial charges on the CH₃ sites. For that case the full $1/r$ potential is used. The rationale for not applying the shifted force in this case is discussed below. Periodic boundary conditions were imposed in all three spatial dimensions. The volume of the system was set so that the water density was 1 g/cm³, and the temperature of the system was maintained at 25 °C by separate Nöse-Hoover thermostats for the translational and rotational degrees of freedom of the solvent.²⁵

At the start of the simulation, the alkane chain was placed in contact with the solvent and the solvent molecules were allowed to adapt to the presence of the alkane before any motion of the alkane was permitted. In this way, the disruption of the solvent due to the presence of the solute was allowed to relax. Once the system was “stabilized”, production runs were made in 50 ps blocks until sufficient statistics had been obtained. As noted below, this required 3–4 ns, so 60–80 blocks were generated.

2.6. Electrostatics. It has been known for some time that spherical truncation of ion–ion, ion–solvent, and solvent–solvent electrostatic interactions results in an artificial interaction at intermediate distances between the ions.^{26,27} We believe that the spherical truncation of electrostatic interactions between the charges on the chain ends and water and urea does not create unphysical attraction between the charged chain ends for the following reasons. The partial charges on the ends of the hydrocarbon chain are considerably smaller than the charges present in the above cases. Moreover, this interaction was not truncated via the shifted force approach to guard against any artificial effect. To support this assertion, we report in the Appendix the potential of mean force (PMF) between two “ions” with charges of +0.2e and –0.2e in water. The absence of artificially generated interactions in the PMF for this test case lends credence to the treatment of the interactions between the partial charges on the chain and the solvent.

3. Results

We performed MD simulations for four systems. Letting HC stand for the 20-mer hydrocarbon chain, they are (I) HC($C = 0$, $q = 0$), (II) HC($C = 6$ M, $q = 0$), (III) HC($C = 0$, $q = \pm 0.2e$), and (IV) HC($C = 6$ M, $q = \pm 0.2e$). In systems III and IV the HC has a positive charge ($q = 0.2e$) at one end of the chain and a negative charge ($q = -0.2e$) at the other. In all cases the chain fluctuates between “two states” (see below). Treating the end-to-end contact formation as an elementary “folding” event, we used MD simulations to monitor the reaction



where **U** is the ensemble of “unfolded” conformations and **N** is the set of conformations in which there is a contact between the chain ends. Following the protein folding terminology, **U** and **N** will be referred to as unfolded and folded states, respectively. The **N** state in our case has residual entropy. Therefore, the set of conformations in which the chain ends are in contact constitute the native basin of attraction (NBA). In systems I and II the **N** state is preferred. The contact formation in systems III and IV is driven by favorable Coulomb interaction between the charges on the chain ends. A snapshot of conformations belonging to the **U** and **N** states is displayed in Figure 1.

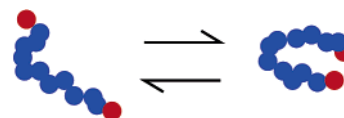


Figure 1. A sketch of the folding reaction monitored using molecular dynamics simulations. Typical structures of the **U** and **N** states obtained in the course of the simulations are shown here. The **N** conformation resembles a fragment of a “helix” more than a planar “hairpin” structure.

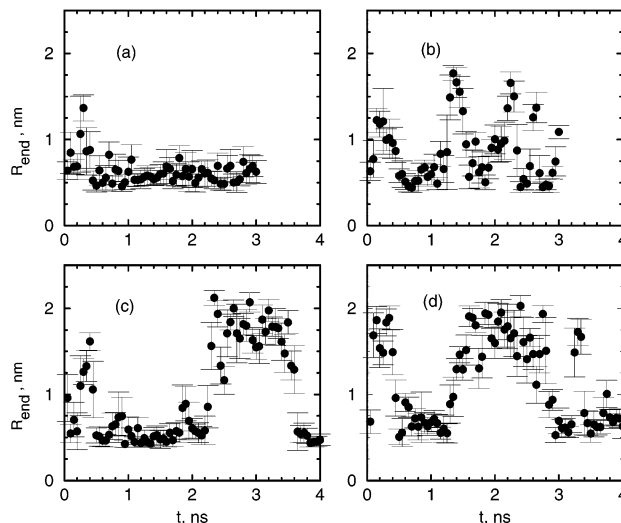


Figure 2. Time dependence of end-to-end distance R_{end} for the four model systems: (a) uncharged hydrocarbon chain in pure water; (b) uncharged HC in 6 M urea solution; (c) charged HC in water; (d) charged HC in 6 M urea solution. These are labeled as systems I–IV in the text. Except in system I, there are multiple transitions between the folded ($R_{\text{end}} \leq R_C$) and unfolded ($R_{\text{end}} > R_C$) states. Despite the lack of specific interactions stabilizing the NBA, the HC behaves like a two-state system.

The simplicity of the folding reaction allows us to use the end-to-end distance, R_{end} (or equivalently the radius of gyration R_g), as an appropriate “order parameter” that distinguishes between **U** and **N**. A contact occurs if $R_{\text{end}} \leq R_C = 7.9$ Å. Thus, the NBA represents the ensemble of conformations with $R_{\text{end}} \leq R_C$. The **U** state is defined by conformations with $R_{\text{end}} > R_C$. Although small changes in R_C do not qualitatively alter our conclusions, the free energy estimates will undoubtedly change. The Lennard-Jones parameters for the nonbonded interactions of the HC are such that R_C cannot be decreased below 7.9 Å.

The fraction of chain molecules that are folded is

$$f_N = \langle \Theta(R_C - R_{\text{end}}) \rangle \quad (3)$$

where $\Theta(x)$ is the Heavyside function. In our simulations the ensemble average is replaced by a time average. This, of course requires that the chain sample enough conformations so that the system is effectively ergodic on the time scale of simulations. The occurrence of several reversible transitions between **U** and **N** during the 4 ns simulations (Figure 2) allows us to estimate, with some confidence, the equilibrium constant for **U** \leftrightarrow **N** using

$$K_{\text{UN}} = (f_N)/(1 - f_N) \quad (4)$$

The time dependence of R_{end} displayed in Figure 2 shows that the **U** \leftrightarrow **N** transitions occur over a relatively narrow time interval so that the ratio of the transition time from **U** \leftrightarrow **N** and the residence time in either state is much less than 1. Therefore, the free energy surface partitions into two basins of attraction corresponding to the **U** and **N** states. Moreover, no long-lived

(24) Haile, J. M. *Molecular Dynamics Simulation: Elementary Methods*; John Wiley and Sons: New York, 1992; pp 192–193.

(25) Martyna, G. J.; Klein, M. L.; Tuckerman, M. J. *Chem. Phys.* **1992**, *97*, 2635.

(26) Huston, S. E.; Rossky, P. J. *J. Phys. Chem.* **1989**, *93*, 7888, 7895.

(27) Bader, J. S.; Chandler, D. J. *J. Phys. Chem.* **1992**, *96*, 6423.

“intermediate” state ($R_C < R_{\text{end}} < R_{\text{max}} \approx 2$ nm) is significantly populated. These observations justify using the “two-state” approximation. It also follows from Figure 2 that even if R_C is increased to 1 nm the estimate of K_{UN} will not change.

The role of finite concentration of solute and possible cooperative effects on the relative stability of the **U** and **N** states is not addressed in this study.²⁸

3.1. Is Urea-Induced Unfolding Caused by Changes in Hydrophobic Interactions? To answer this question, we consider urea-induced transitions in systems I and II. The absence of charges eliminates any electrostatic interaction between the HC and urea (or water). Thus, chain unfolding can occur *only by alterations in urea-induced hydrophobic interactions*. The time dependence of $R_{\text{end}}(t)$ (Figure 2a) for system I shows that the **N** state is preferred in water. For $t > 0.5$ ns, R_{end} is pinned around 6 \AA ($< R_C$). There are minor fluctuations around $R_{\text{end}} \approx 6 \text{ \AA}$. The equilibrium constant $K_{\text{UN}} \approx 12$, which implies that the **NBA** is dominantly populated. The stability of the **N** state with respect to **U** is $\Delta F_{\text{UN}} = (F_{\text{N}} - F_{\text{U}}) = -RT \ln K_{\text{UN}} \approx -1.5$ kcal/mol.

The equilibrium between **U** and **N** shifts in the presence of 6 M urea. For system II we find (Figure 2b) that the chain makes several transitions to the **U** state in the course of the 4 ns simulations. Thus, the HC samples conformations belonging to **NBA** and the **U** state. From the histogram of R_{end} we estimate $K_{\text{UN}} \approx 2.3$, which implies that $\Delta F_{\text{UN}} \approx -0.5$ kcal/mol. Although the **N** state is destabilized by about 1.0 kcal/mol in 6 M urea, the **NBA** is still preferentially populated. The higher solubility of the 20-mer hydrocarbon chain in aqueous urea solution is in accord with the well-known observations that urea diminishes the hydrophobic effect. However, in this system the effect is not large enough to unfold the chain.

3.2. “Denaturation” Is Dominated by Electrostatically Mediated Interactions. The HC with charges at the ends (systems III and IV) accounts for modest electrostatic effects and hydrophobic interactions. This model, which accounts for chain conformational entropy, is one of the simplest for which MD simulations can be used to probe the mechanism of denaturation by urea. In polypeptide chains, in which a multitude of interactions can be effected by urea, it is difficult to estimate the contributions that different amino acids make to the destabilization free energy. In contrast, in our model unfolding (increase in R_{end}) of HC can only occur if urea preferentially solvates the charges at the ends of the chain. Because only the ends of the chain have small partial charges, the bulk of the interactions between the chain and the solvent are hydrophobic in nature. Thus, with these systems we are able to isolate the hydrophobic and electrostatic contributions to urea-induced chain destabilization.

The dynamics of $R_{\text{end}}(t)$ (Figure 2c) for system III (no urea) shows that there are frequent transitions between **N** and **U**. The Coulomb attraction between the charges on the chain ends is not sufficient to stabilize the chain in the **NBA**. The **N** state for system IV is destabilized because the gain in electrostatic energy due to charge–urea interactions is greater than the favorable interactions between the opposite charges on the ends of the chain. Given that ΔF_{UN} for system III is ~ -0.4 kcal/mol (comparable to system II), it follows that the **N** state is still

more stable, albeit marginally. The marginal stability of the HC in system III arises from a competition between the favorable Coulomb interaction between the charges on the chain ends and the electrostatic interaction between water and the charges on the HC. Apparently, the small value of q only marginally stabilizes the **N** state. If this value is increased to $q = \pm 0.8e$, we find that the **N** state is so overwhelmingly stable that even 6 M urea does not readily unfold the chains.

In contrast to the above situation the addition of 6 M urea to system III results in the breakup of chain ends, leading to the transition from **N** to **U**. The chain visits the **U** state for a greater duration than the **NBA** (Figure 2d). The free energy $\Delta F_{\text{UN}} \approx 0.1$ kcal/mol, which suggests that 6 M urea may correspond to roughly the midpoint of the **U** ↔ **N** transition for this system. The results for system IV give a preliminary indication that electrostatic interactions between urea and the charges on the chain ends are the primary factors in unfolding the HC.

The effect of the charges on the chain in shifting the equilibrium to the **U** state can be quantitated using the ΔF_{UN} values for the four systems. An estimate of the destabilization of **N** due to hydrophobic interaction alone is

$$\Delta\Delta F_{\text{HC}} = \Delta F_{\text{UN}}(C = 6 \text{ M}, q = 0) - \Delta F_{\text{UN}}(C = 0, q = 0) \quad (5)$$

Using the ΔF_{UN} values from systems I and II, we find that $\Delta\Delta F_{\text{HC}} \approx 0.9$ kcal/mol. In other words, the contribution to destabilization of the **N** state of the hydrocarbon carbon per methylene group is only about 0.05 kcal/mol. Similarly

$$\Delta\Delta F_{\text{CHC}} = \Delta F_{\text{UN}}(C = 6 \text{ M}, q = \pm 0.2e) - \Delta F_{\text{UN}}(C = 0, q = \pm 0.2e) \quad (6)$$

is 0.5 kcal/mol. **CHC** refers to the charged case. If the interactions due to changes in hydrophobic and charge effects are additive, then the contribution to the destabilization of the **N** state for one of the charges in the chain is about 0.25 kcal/mol. This is about 5 times larger than the effect due to changes in the urea-induced hydrophobic interactions. The additivity assumption is likely to be reasonable because in the present system electrostatic interactions between chains are a relatively small perturbation. For example, at $R_{\text{end}} \approx 7 \text{ \AA}$ the attractive Coulomb interaction between the chain ends is about 0.024 kcal/mol. An alternative way of viewing the urea-induced electrostatic interaction is to compare systems II and IV. In this case $\Delta\Delta F = \Delta F_{\text{UN}}(C = 6 \text{ M}, q = \pm 0.2e) - \Delta F_{\text{UN}}(C = 6 \text{ M}, q = 0) \approx 0.6$ kcal/mol. Both approaches show that the electrostatic interaction between urea and the **CHC** destabilizes the **N** state. Thus, the introduction of even modest charges on the ends of the chain dramatically alters the urea-induced unfolding transitions of the model system. These simulations show that the predominant denaturation action of urea is electrostatic in origin *even in a system that has a large contiguous patch of hydrophobic moieties*. By patch we mean that in both the **U** and **N** states there is a large hydrophobic surface area exposed to the solvent. The exposed surface area is $\sim R_G^2$, which is on the order of 300 and 70 \AA^2 in the **U** and **N** states, respectively.

The estimated free energy differences are small but are in line with the measured stabilities of folded states of globular proteins (see the Introduction). In light of the truncations used in treating the interaction between the hydrocarbon charges and

(28) Franks, F. *Water, A Comprehensive Treatise*; Plenum Press: New York, 1975; Vol. 4, pp 45–46.

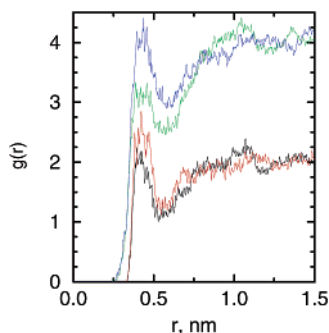


Figure 3. Distribution of water around the ends of the chain for system I. The HC is uncharged, and the urea concentration is zero. The curves in red and black are for the distribution of O around the two chain ends. The blue and green curves represent pair functions between hydrogen atoms and the chain ends.

water and urea the small value could be a source of concern. It has been pointed out that incorrect treatment of electrostatic interactions can introduce an artificial repulsion at large distances between unlike charges.²⁶ We show in the Appendix that artificial repulsion is not exhibited by the potential of mean force for ions in water when the ion charges are $\pm 0.2e$ and the interactions are truncated by the shifted force method. This gives us confidence in the estimates of the equilibrium constants for the charged HC.

4. Urea Depletes Water Molecules around the HC

4.1. Uncharged Hydrocarbon Chains. To obtain a microscopic picture of how urea induces global conformational changes in the HC, we computed several pair correlation functions involving water, urea, and the HC. To assess the plausible changes in water structure, we use system I as the reference state. In the absence of urea and charges on the chain ends, the HC is in the **N** state with the end-to-end distance pinned at $R_{\text{end}} \approx 3.5 \text{ \AA}$ (Figure 2a). The pair functions between the O and H atoms of water and the chain ends (Figure 3) show that water solvates the CH_3 ends. Both $g_{\text{HC}_E}^{\text{W}}(r)$ and $g_{\text{OC}_E}^{\text{W}}(r)$ (the label E stands for the chain ends) show a pronounced first peak and a rather weak second peak. This suggests that a maximum of up to two layers of water molecules may surround the collapsed HC. Note that the first peak is at a distance that is greater than the Lennard-Jones minimum between C and O atoms. This suggests that the density of water near the chain ends is less than it is in the bulk (see below). Such an effect is not observed in smaller alkanes.¹⁶

In the presence of 6 M urea, the HC fluctuates between **U** and **N**, with the **N** state being preferentially populated (Figure 2b). Comparison of $g_{\text{HC}_E}^{\text{W}}(r)$ and $g_{\text{OC}_E}^{\text{W}}(r)$ in the presence and absence of urea (Figures 3 and 4a) shows that water is less structured around the HC when $C = 6 \text{ M}$. The structure of water in 6 M urea depends on the conformational state of the HC. When the chain is in the **N** state, there is a slight depletion of water around the HC, leading to a minor perturbation (compared to system I) of water structure around CH_3 . At short values of R_{end} the two CH_3 groups cannot accommodate water molecules. As a result there is a distortion of the water structure when the HC is in the **NBA**. However, when the HC is in the **U** state ($R_{\text{end}} \geq 7.9 \text{ \AA}$), there is a well-defined water solvation shell (Figure 4b) because the ends of the chain can be “solvated” by water without possible overlap between the methyl groups.

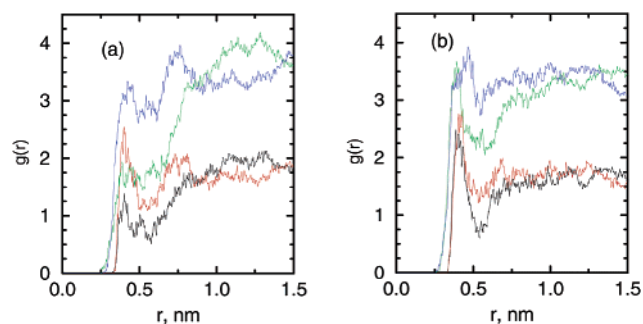


Figure 4. (a) Same as Figure 3 except the urea concentration is 6 M. The HC is in the native basin of attraction (NBA). (b) Conditions the same as in (a) except the HC is unfolded.

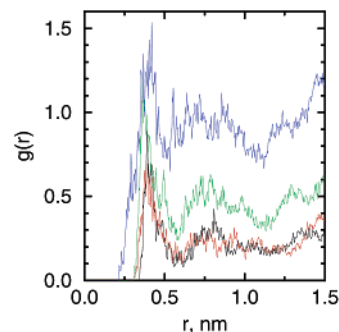


Figure 5. Pair functions between the atoms in urea and the methyl groups at the ends of the unfolded HC in the presence of 6 M urea. The black, red, green, and blue curves correspond to the distribution functions between the chain ends and C, O, N, and H, respectively.

Urea preferentially solvates the methyl groups of the HC, which is consistent with the well-known observation that solubilities of hydrophobic residues increase in aqueous urea solutions. The pair correlation functions between urea and the chain ends (Figure 5) show a single peak in O, N, and C of urea. The peak is most prominent in the pair function involving the nitrogen atom and the HC chain ends, which suggests that urea is structured with nitrogen oriented toward the carbon of the HC. Because the interactions between urea and HC, in the absence of charges on the chain ends, is a weak Lennard-Jones potential, we do not observe significant ordering of the cosolute urea around the HC.

In all pair functions there is considerable asymmetry of the solvent structure around the chain ends. This somewhat unexpected behavior is a consequence of the HC not being spherical even in the collapsed state. The asphericity of the chain is reflected in the inequality of the three principal radii of gyration.

4.2. Charged Hydrocarbon Chains. The depletion effect, which is only moderately observed in the uncharged HC, becomes dramatic when the chain ends are charged (systems III and IV). Consider system III, which corresponds to the HC with charges in pure water. The **NBA** is only marginally more stable than the **U** state. The structure of water around the chain ends (Figure 6) is qualitatively the same in both the **U** and **N** states. The pair functions show that there is a layer of water around the HC. Surprisingly, there is *symmetry* in the O and H atom distribution functions with respect to the two oppositely charged ends. Naively, we would expect that the negatively charged O would orient preferentially toward the $+q$ end and the positively charged H would point toward the $-q$ end. This

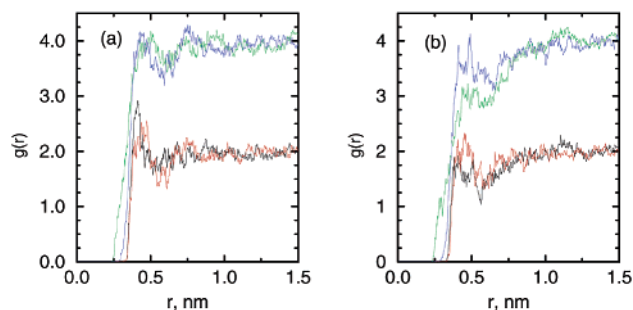


Figure 6. (a) Distribution functions between O and H of water and the two charges on the chain ends in the absence of urea. The black and red curves represent $g_{O-q}(r)$ and $g_{O+q}(r)$, respectively, while the green and blue curves correspond to $g_{H-q}(r)$ and $g_{H+q}(r)$, respectively. The HC is in the unfolded state. (b) Same as in (a) except the HC is in the NBA.

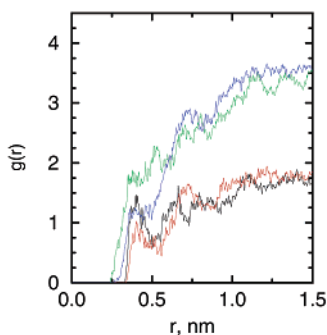


Figure 7. Pair functions involving water and the charges on the ends of the chain in 6 M aqueous urea solution. The chain is in the NBA. The depletion effect (lack of water density around the chain ends) is dramatically illustrated.

is the case in the solvation of ions (Na^+ and Cl^-)²⁹ in pure water where the favorable Coulomb interactions are largely responsible for the hydration energy. In the present situation the repulsive energy between O and $-q$ is $V_R = qOq/4\pi\epsilon_{\text{eff}}R$. If we use a value in the range 5–10 for the effective dielectric constant ϵ_{eff} and $R \approx 5 \text{ \AA}$, then we find that $V_R \approx (1.8 - 3.6)k_B T$. This is relatively a small penalty to pay to nearly preserve the hydrogen bond network around the chain ends of the HC.

There is substantial depletion of water around the charged ends in 6 M aqueous urea solution. Comparison of the water pair function around the ends of the HC in water (Figure 6b) and 6 M urea solution (Figure 7) shows that urea dramatically decreases the density of water. Interestingly, the second peak in $g_{O+q}(r)$ and $g_{O-q}(r)$ grows slightly in 6 M urea, suggesting that the depleted water has been displaced by about 5 \AA . The depletion effect further establishes that the denaturation due to urea is *almost entirely electrostatic* in origin.

The depleted hole created by water is occupied by urea molecules that preferentially solvate the charged chain ends. In the U state, which is favored slightly in 6 M urea, the solvation of $+q$ by urea is greater than that of $-q$ (Figure 8). This is because the N atom in urea carries a charge of $-0.542e$ and the favorable electrostatic interaction orients the N atoms toward the $+q$ end (Figure 8). Because of charge effects, there is substantial asymmetry in the arrangement of urea around the two chain ends. The detailed examination of the structure of the solvent around the HC establishes that urea-driven depletion of water, which leads to direct electrostatic interaction between

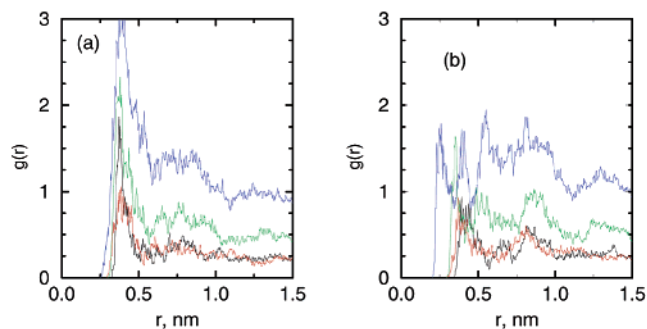


Figure 8. (a) Distribution of urea around the $+q$ charge in 6 M urea solution. The black, red, green, and blue curves are for C, O, N, and H, respectively. The chain is in the NBA. (b) Same as in (a) except the curves represent pair functions between urea and the $-q$ charged end.

urea and the charges on the HC, is the major driving force in causing the $U \leftrightarrow N$ transition in this model system.

4.3. Urea-Induced “Dewetting” near the HC. The accommodation of large nonpolar solutes is difficult because a substantial number of hydrogen bonds have to be broken. Thus, it is natural to suggest that the very nature of the effective hydrophobic interaction might change as the dimensions of the solute become larger; i.e., the hydrophobic interaction is scale dependent.^{30,31} Dewetting (substantial reduction in water density) around a large hydrophobic wall has been observed in constant-pressure simulations of a pair of interacting oblate ellipsoids.³² These simulations suggest that the very nature of the hydrophobic interaction might change if the solute dimension is on the order of 10 \AA . The radius of gyration R_g of the HC is between 8 and 18 \AA depending on the state of the HC. In the collapsed state the Flory estimate is $R_g \approx \sigma N^{1/3} \approx 8.3 \text{ \AA}$. Because the HC has a contiguous patch of hydrophobic residues, we expect to see remnants of a “drying”-like transition.

We computed the pair functions $g_{CO}(r)$, where O is the oxygen atom of the water molecules and C is a carbon atom of the HC. To probe the water structure around the whole chain, we averaged over all the carbon atoms of the HC. From the pair functions for system II (HC has charges on the chain ends, and the urea concentration is zero) we find only mild structuring of water around the HC as indicated by a small first peak. The peak height for the chain in the U state is larger than for a chain in the N state (compare the two curves in Figure 9a). Nevertheless, there is a suppression of water molecules around the HC regardless of whether it is expanded or collapsed.

The depletion effect is *dramatic* in the presence of urea. In this case, there is *absence* of water molecules near the HC (Figure 9b). The density near the HC is less than in the bulk. These curves show, in a spectacular manner, that urea drives the water molecules away from the HC that contains a stretch of hydrophobic moieties. This effect is independent of the chain conformation. However, just as for system III, we find that the effect is stronger when the chain is in a globular conformation (see the suppression in the water structure when the chain is in the NBA, Figure 7). The mild dewetting observed in these cases is not inconsistent with the structure of water near alkane chains in the presence of modest solute–solvent attraction.³³

(30) Stillinger, F. H.; *J. Solution Chem.* **1973**, *2*, 2141.

(31) Lum, K.; Chandler, D.; Weeks, J. D. *J. Phys. Chem. B* **1999**, *103*, 4570.

(32) Wallqvist, A.; Berne, B. J. *J. Phys. Chem. B* **1999**, *99*, 2983.

(33) Huang, D. M.; Chandler, D. *J. Phys. Chem. B* **2002**, *106*, 2047.

(29) Mountain, R. D. *Int. J. Thermophys.* **2001**, *22*, 101.

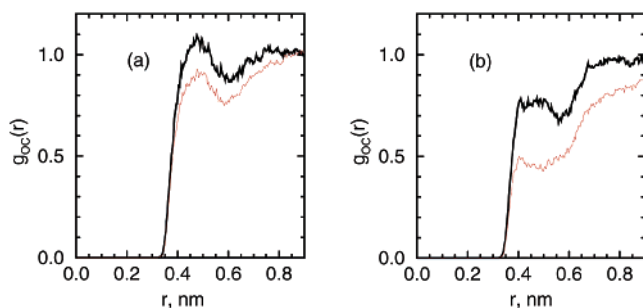


Figure 9. Pair correlation functions $g_{OC}(r)$ between the oxygen atom of water and the carbon centers of the HC averaged over all 20 HC carbon atoms. The black lines correspond to the case when the chain is in the U state, and the red lines are for the HC in the N state. Panel (a) is for system III (charged HC with no urea), and panel (b) is for system IV (charged HC in 6 M urea). The dramatic effect of urea-induced depletion of water is evident.

5. Conclusions

The primary finding of this paper is that urea denaturation occurs predominantly by an electrostatic mechanism. This has been clearly shown in model hydrocarbon systems for which converged molecular dynamics simulations can be undertaken. Using four variants of a long hydrocarbon chain in water, we have shown that the direct interaction with the charges is the major determinant of urea denaturation. In the case when the ends of the chain carry a modest charge ($+0.2e$ at one end and $-0.2e$ at the other) urea directly solvates the chain ends. This effectively destabilizes the collapsed chain so that the contact formed in the absence of urea is broken in 6 M urea solution. Remarkably, this *specific binding* dominates in a system that has a large contiguous (on the order of 10 \AA) hydrophobic patch. If the hydrophobic mechanism were dominant, a significant shift in the equilibrium to the unfolded state would have occurred for the *uncharged HC* in 6 M urea. The simulations show that the free energy of destabilization due to urea-induced hydrophobic interaction is too small. This observation and direct microscopic analysis of the urea structures show that urea denaturation is dominated by an electrostatic mechanism, with the hydrophobic mechanism playing a relatively minor role. The direct binding of urea to the charged ends leads to the depletion of water around the HC.

The proposed mechanism of urea action has, in retrospect, considerable experimental support beginning with the classic work of Robinson and Jencks.⁵ By studying the solubility of acetyltetraglycine ethyl ester (ATGEE) in aqueous urea solution (and other denaturing agents), they suggested that urea interacts directly with the peptide backbone by forming hydrogen bonds. Although their study was not conclusive, they postulated that a specific electrostatic interaction of urea with ATGEE leads to its enhanced solubility in urea solution. More recent calorimetric studies³⁴ of protein denaturation have also been interpreted using direct binding, in the form of favorable hydrogen bond formation, between urea and the charged (or polar) residues.

Although the HC studied in this paper is a relatively large flexible molecule, which displaces a large number of water molecules due to excluded volume, the structure of the water is not significantly perturbed. The changes in water structure are mostly confined to a layer of water around the solute. This is in accord with simulations of interacting oblate ellipsoids in

water.³² The depletion-induced attraction is due to the release of the interfacial water molecules that causes dewetting. The resulting attraction is due to osmotic pressure on the platelets. In the HC system, we find some remnant of loss of water density near the HC (an effect not observed in smaller alkanes¹⁶) regardless of whether the chain is in the U or the N state. The chain collapses in water because the increase in the energy due to *gauche* defects is compensated by many favorable van der Waals intramolecular interactions. Thus, in contrast to the interellipsoid attraction, whose origin is entropic, both enthalpy changes and entropy changes contribute to chain collapse in water.

Our simulations suggest that the urea denaturation occurs by an “outside-in” action that leads to a two-stage urea-induced protein unfolding mechanism.⁶ In the initial stage a natively like intermediate should form. In such a structure there is direct interaction between urea and the solvent-exposed residues. The core of the protein could be intact. Such a state, which may be hard to detect experimentally, could be followed by global unfolding in which both side chain contacts and the hydrogen bond network are disrupted. The highly natively like intermediate formed upon initial interaction of urea with the exposed polar groups and peptide bonds could be termed a “dry” intermediate (low density of water near the protein). The proposed mechanism of urea-induced unfolding suggests that a denaturant-induced unfolding mechanism populating a kinetic natively like intermediate could be universal. Experiments of GuHCl unfolding of ribonuclease A³⁵ show that such an intermediate does exist. The early formation of such a dry natively like structure follows from the electrostatic denaturation mechanism and cannot be easily explained if urea-induced unfolding occurs because of changes in the hydrophobic interactions. Detection of kinetically generated natively like intermediate using “urea-jump” experiments would be invaluable in shedding light on the denaturation mechanism.

6. Appendix

In our simulations the electrostatic interactions between the charges on the ends of the HC and solvent molecules (water and urea) are truncated using

$$V_T(r) = V(r) - V(r_c) - (r - r_c) \left. \frac{dV}{dr} \right|_{r_c} \quad (\text{A1})$$

This truncation is different from the spline truncation used in the literature previously cited,^{26,27} where the use of truncation leads to artificial features in the potential of mean force, $W(r)$, between charges. This might imply that such artifacts could have introduced biases in the sampling of the charged HC conformations in our simulations. Such a bias would call into question our estimates of the urea-dependent equilibrium constants between the folded and unfolded conformations. The purpose of this appendix is to show that there are no artificial features in $W(r)$ between the charges $+0.2e$ and $-0.2e$ when the shifted force truncation is employed. The PMF was calculated using standard procedures at ambient water density. The MD simulations were carried out using 998 water molecules and the two charges. Each window was equilibrated for 20 ps before a 20 ps duration sample was obtained. The computed PMF (Figure

(34) Makhatadze, G. I.; Privalov, P. L. *J. Mol. Biol.* **1992**, *226*, 491.

(35) Kiefhaber, T.; Labhardt, A. M.; Baldwin, R. L. *Nature* **1995**, *375*, 513.

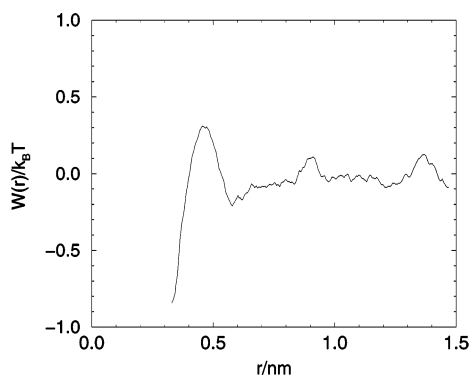


Figure 10. Potential of mean force, $W(r)/k_B T$, for the case with partial charges $+0.2e$. The value of the cutoff for the shifted force is $r_c = 0.948$ nm. The structure beyond 0.8 nm is probably an indication of the noise in the simulation.

10) shows that $W(r) = 0$ for $r \geq r_c$ in accord with eq A1. If there were artifacts, as found elsewhere, then $W(r)$ would deviate

from zero starting from r close to r_c . The absence of artificial repulsive forces between unlike charges in our simulation may be due to (i) small values of the charge, (ii) the relatively large number of water molecules, and (iii) smooth truncation of the long-range interaction. In any case, this calculation shows that the treatment of electrostatic interactions involving the charged HC used here does not bias the conformational sampling. This in turn gives us confidence in the estimated equilibrium constants for the charged HC.

Acknowledgment. We have benefited from discussions with R. Elber. James Sims converted our serial code into the parallel processing version used in these simulations. We thank David Chandler and Lawrence Pratt for their interest in this work. This work was supported in part by a grant (to D.T.) from the National Science Foundation (CHE 029340).

JA020496F